

The Effects of Anisotropic Free-Stream
Turbulence on Turbulent Boundary Layer
Behavior



Fang Liang-Wei
Jon A. Hoffman

THE EFFECTS OF ANISOTROPIC FREE-STREAM
TURBULENCE ON TURBULENT BOUNDARY LAYER
BEHAVIOR Report, 1 Jul. 1984 - 1 Jul. 1985
(California Polytechnic State Univ.) 43 p
HC A03/MF A01

N86-16192

Unclas

CSSL 01A G3/02 03669

CONTRACT NSG-2391
November 1985

NASA

NASA CONTRACTOR REPORT 177379

Fang Liang-Wei
Nanjing Aeronautical Institute
Peoples Republic of China

Jon A. Hoffman
Aeronautical Engineering Department
California Polytechnic State University
San Luis Obispo, CA 93407

Prepared for
Ames Research Center
Under Grant NSC 2381



National Aeronautics and
Space Administration

Ames Research Center
Moffett Field, California 94035

ABSTRACT

The effects of near-isotropic and highly anisotropic free-stream turbulence on mean flow properties and properties of the turbulent structure of turbulent boundary layers in a near zero pressure gradient flow has been experimentally evaluated. Turbulence levels varied from 0.5% to 8.0% and the momentum thickness Reynolds number varied from 800 to 1100.

The results indicate that the effects of free-stream turbulence on the classical boundary layer properties for near-isotropic turbulence which have been published by other investigators are similar to the case of highly anisotropic turbulence fields, while the effects of free-stream turbulence on the properties of the turbulent structure within the boundary layer for the case of near-isotropic turbulence are quite different compared to the highly anisotropic case.

INTRODUCTION

Turbulent boundary layers or other shear layers generated in engineering generally lie beneath a significantly turbulent stream. A good example is the flow in a multistage axial turbomachine, in which the disturbances felt by the boundary layers on the blades of one of the later rows include: (1) periodic unsteadiness due to the rotating wakes of upstream stages; (2) periodic strong bursts of turbulence due to the wakes of the blades in the preceding few rows; and (3) circumferentially homogeneous and anisotropic turbulence generated by the blade rows far upstream.

The free-stream turbulence levels encountered in practical fluid flow problems can vary over a wide range. The turbulence levels in free flight are very much less than 1% whereas the flow in turbomachines may have turbulence levels as high as 8% to 10%. When the free-stream turbulence scale is much larger than that of a turbulence shear layer (or boundary layer thickness), the boundary layer may be considered to experience an unsteady external flow; for this case, Parikh (1) has shown that the time averaged velocity profile is the same as the velocity profile with a steady external flow. Turbulence with a scale much smaller than that of a shear layer decays rapidly and has no practical relevance. Only turbulence with scales of the same order as the thickness of the shear layer have been found to exert a significant effect on the mean properties of the shear layer.

The effect of turbulence level on boundary layer behavior has not gone unnoticed; recent published papers relate to the idealized nearly-homogeneous

nearly-isotropic turbulence case and have mainly been restricted to boundary layers without pressure gradients. Investigations by Kline (2), Huffman (3), Meier (4), and recent papers by Hancock (5), Raghunathan (6), and Castro (7) have shown that the boundary layer skin-friction and the integral properties of the boundary layer are very sensitive to the free-stream turbulence level for $\sqrt{q'^2}/U_m \geq 1\%$, and may be unaffected at lower intensities of turbulence. Investigations by other authors were performed with nearly homogeneous, nearly isotropic turbulence and the influence of isotropy on the above interaction is not yet understood. This is particularly important for a multistage axial turbomachine; as mentioned previously. Sullery (8) investigated the free-stream turbulence effects on compressor cascade wakes. His results indicated that the wake decay is faster for the case of high free-stream turbulence levels and the drag coefficient decreased slightly as the turbulence level was increased. Sullery's results, however, were limited to $\sqrt{q'^2}/U_m \leq 2.78\%$ which is much lower than the turbulence levels generated by a compressor in a turbomachine.

The present paper will document some of the effects of free-stream turbulence on the integral properties of turbulent boundary layers and properties of the turbulent structure in a near zero pressure gradient flow. The turbulence level range investigated varies from 0.5% to 8%. Attention is concentrated on cases when the free-stream turbulence fields are near-isotropic (generated by grid sets) and anisotropic (generated by rod sets with a significant downstream flow contraction).

NOMENCLATURE

Symbols

b	= channel height
b_o	= rod length
B	= strip width of the grids sets
C	= channel length
c_f	= skin friction coefficient = $\tau_w / \rho U_m^2 / 2$
D	= rod diameter
H	= shape factor of boundary layer = δ^* / θ
k	= turbulent kinetic energy = $(\overline{u'^2} + \overline{v'^2} + \overline{w'^2}) / 2$
M	= mesh size of the grid sets and rod sets
n	= number of grid set strip or rods
$\sqrt{q'^2}$	= total RMS turbulence quantity = $\sqrt{(\overline{u'^2} + \overline{v'^2} + \overline{w'^2})} / 3$
r	= radius of rod set geometry
Re_{W1}	= Reynolds number based on channel width = $U_m W_1 / \nu$
Re_θ	= momentum thickness Reynolds number = $U_m \theta / \nu$
R_x	= free-stream autocorrelation coefficient in flow direction at diffuser inlet
R_y	= free-stream cross-correlation coefficient in y direction at diffuser inlet
s	= gap between grid sets and inlet section
U_m	= average free-stream velocity in flow direction
\bar{U}	= mean velocity in flow direction
U_τ	= shear velocity = $\sqrt{\tau_w / \rho}$
U^+	= non-dimensional velocity = \bar{U} / U_τ
u', v', w'	= turbulence component velocities

Symbols

W_1	= channel width
x, y, z	= cartesian coordinates
y^+	= non-dimensional distance = $U\tau y/\nu$
δ	= boundary layer thickness
δ^*	= boundary layer displacement thickness
θ	= boundary layer momentum thickness
λ_x	= free-stream integral scale of turbulence in x direction
λ_y	= free-stream integral scale of turbulence in y direction
τ_w	= wall shear stress
ρ	= fluid density
ν	= kinematic viscosity
Δc_f	= fractional change in skin friction
ΔH	= fractional change in shape factor

Subscript

o	= value in absence of turbulence generating grid or rod
-----	---

EXPERIMENTAL PROGRAM

Experimental Apparatus

The experimental system used for the investigation, shown in Fig. 1, consists of a base-plate and top-plate for upstream rods and grids, a throat, a straight channel, a plenum chamber, a fan and a noise attenuator. The fluid, air, is drawn through the system with a five horsepower centrifugal fan. The flow rate is controlled by adjusting a throttle which is located between the exit section of the fan and the inlet section of the noise attenuator. Screens and filters located in the plenum are used to improve flow conditions at the fan inlet.

Throat and Straight Channel

The straight channel was constructed out of clear lucite; the channel width dimension (W_1) is 26 mm. The channel height/inlet width ratio (b/W_1) is 5.86 and the channel length/inlet width ratio (C/W_1) is 4.88. In the channel, boundary layers develop. The channel has four pressure taps located upstream of the channel exit section. The throat of the straight channel has an ASME standard nozzle shape. Masking tape applied to the throat caused transition from a laminar to a turbulent boundary layer to begin at the location of the tape rather than randomly along the channel walls. The measuring station was located at 1 mm upstream of the channel exit section. The Reynolds number, based on the width of the channel, is 7.8×10^4 .

Turbulence Generation

Rods and grids used for turbulence generation were placed between the base-plate and top-plate upstream of the throat as illustrated in Figs. 1 and 2.

The rod length/channel height ratio was fixed at 1.71 for all rod sets. All grids were rectangular-mesh rectangular-bar biplane grids except for one which was a commercial screen. A gap between the grid sets and the face of the inlet channel (S) is shown in Fig. 1. Geometrical information about all upstream rod sets and grid sets are presented in Table 1.

Instrumentation and Data Processing

The primary data record in the experiments were velocity profiles in the boundary layers, turbulence levels, auto and cross correlation coefficients (used to obtain turbulence length scales), and Reynolds stress measurements. Wall skin friction was measured with a Preston tube using the calibration table of Head et al., (9). The Preston tube was also used as a pitot tube for boundary layer velocity profiles measurements. Turbulence measurements were obtained by using two model 1010A T.S.I. constant temperature hot wire anemometers, two model 1005B linearizers, a model 1015A correlator, two model H.P. 3400A true rms meters and a T.S.I. 1076 true rms meter. In order to obtain turbulence quantities averaged for 10 second periods, the d.c. output from the rear panel of the rms meter was fed into a H.P. 2212A voltage to frequency converter and then into a H.P. 5223L electronic counter. A Tektronix dual beam oscilloscope was used to monitor the turbulence signal.

The turbulence levels in the streamwise direction were obtained using single hot wires mounted in a micrometer traversing device. Free-stream turbulence levels in the y and z directions were obtained by using probes with single wires inclined 45° to the mean stream direction. Free-stream longitudinal correlation coefficients were obtained using a single hot wire placed normal to the flow. Values of the longitudinal integral scales of

turbulence (λ_x) were obtained by integration of the area under curves of the longitudinal correlation coefficient (R_x) versus a distance corresponding to the time delay of the hot wire signal (Taylor's hypothesis). Cross correlation coefficients (R_y) were obtained using probes with two parallel wires (the wires being displaced by different distances) along with a 1015A correlator. Lateral integral scales (λ_y) were then obtained by integrating the area under curves of R_y versus the distance between the wires. Reynolds stress profiles in boundary layers were measured by using an x hot wire probe along with the correlator taking the (A-B) rms value and mean value from linearizers.

A flattened pitot tube (or Preston tube) with tip outside and inside dimensions, measured in the y direction, of 0.3 mm and 0.15 mm respectively, was mounted on a Unislide traversing mechanism whose position accuracy was better than 0.025 mm. Inclined manometers were used for all pressure measurements. A pressure loss coefficient across the rods and grids was experimentally obtained for each rod set and grid set. This pressure loss, along with a pressure differential between the pressure from taps located in the top-plate and base-plate upstream of the rods, and the pressure from static taps located upstream of the channel exit, was used to determine the free-stream channel velocity.

RESULTS AND DISCUSSION

The Effects of Free-stream Turbulence on the Classic Boundary Layer Properties

Hot wire spectra of free-stream turbulence at the measuring station are shown in Fig. 3. Discrete peak values were not detected from the signal indicating that the periodical vortices shed by the rods have decayed to random turbulence. Therefore, the hot wire measures a real free-stream random turbulence. Isotropy occurs primarily due to the flow contraction downstream of the turbulence generator.

Nondimensional velocity profiles for various levels of turbulence are shown in Fig. 4. An increase in the free-stream turbulence results in flatter velocity profiles implying an increase in the momentum transport across the boundary layer. Fig. 5 shows nondimensional velocity profiles for both isotropic and anisotropic free-stream turbulence at approximately the same turbulence level. It shows that the velocity profile for anisotropic free-stream turbulence is slightly more full compared with isotropic turbulence.

The influence of free-stream turbulence on boundary layer thickness (δ) is shown in Fig. 6. The variation of δ is nonlinear. The influence of anisotropic turbulence on δ , however, is a little bit larger than for an isotropic turbulence field. The results from Fig. 5 and Fig. 6 imply that the momentum transport across the boundary layer for anisotropic turbulence is a little bit stronger than for the case of an isotropic turbulence field at the same free-stream turbulence level.

The combined effect of the flattening of the velocity profile and the increase in δ results in significant changes in the nondimensional integral properties of the boundary layer shape factor (H) as shown in Fig. 7. The trends of the present results are the same as those of other published papers (4) (6).

The influence of free-stream turbulence on the nondimensional shape factor $\Delta H/H_0$ with three values of $\sqrt{v'^2}/\sqrt{u'^2}$ are shown in Fig. 8, along with the results of Raghunathan (6) and Kline (2). The present results are in close agreement with the other investigators. The results also show that there is no noticeable difference between the highly anisotropic and near-isotropic turbulence cases.

The law of the wall and the law of the wake in the boundary layer are shown in Fig. 9. The skin friction coefficients (c_f) for these plots are based on Preston tube measurements. The plots show that the law of the wall of the form $U/U_\tau = A + B \log (U_\tau y/\nu)$ holds good for all values of free-stream turbulence, confirming that the law of the wall is unaffected by the change in free-stream turbulence. The law of the wake (outer layer), however, is very sensitive to free-stream turbulence level. The strength of the wake component is seen to decrease when the free-stream turbulence level increases, but it is not very sensitive to the isotropy ratio of the turbulence field (Fig. 10).

The influence of free-stream turbulence level on c_f and $\Delta c_f/c_{f0}$ can be observed from Fig. 11. The increase in turbulence level results in an increase in c_f and $\Delta c_f/c_{f0}$. The curve shows nonlinear effects at turbulence levels lower than 4% which is in agreement with the experimental data represented by a curve fit $(\Delta c_f/c_f = 12.6(\sqrt{q'^2}/U_m)^{1.4}$ of data from Raghunathan (6).

Hancock (5) found a linear correlation between the increase in skin friction and decrease in shape factor. The one-to-one correspondence between changes in c_f and changes in the profile shape factor H obtained in this study is consistent with Hancock's result as shown in Fig. 12.

Hancock (5) also reviewed the extensive literature and undertook some particularly careful experiments designed to extend the previously rather limited range of turbulence length scale ratios. His results showed that the effect of free-stream turbulence (nearly isotropic) depends significantly on both the free-stream level and the length scale ratio. His data clearly demonstrates that not only does the effect of free-stream turbulence increase with increasing turbulent intensity but also that the effect decreases with increasing length scale ratio. A simple empirical correlation was found by Hancock that relates the increase in skin friction $\Delta c_f/c_{f0}$ at constant Re_θ (momentum thickness Reynolds number) to a free-stream turbulence and length scale combined parameter $(\sqrt{u'^2}/U_m)/(\lambda_x/\delta + 2)$. Hancock limited his study to values of Re_θ in excess of 2000 in order to avoid serious Reynolds number effects.

Recently, Castro (7) extending Hancock's work to low momentum thickness Reynolds numbers, $Re_\theta \approx 1000$. Castro's results showed that "direct Reynolds number effects are significant and such effects reduce as the level of free-stream turbulence rises."

The range of Re_θ of the present experiment varies from 800 to 1100. Obviously, a Reynolds number effect should exist. In order to check the present results to look at both the effects of length scale and Reynolds number, extensive free-stream turbulence length scale measurements were

obtained by using a single hot wire along with a correlator. The $\Delta c_f/c_{f0}$ versus $(\sqrt{u'^2}/U_m)/(\lambda_x/\delta + 2)$ interdependence is shown in Fig. 13. Castro's results are also shown in the plots. It can be seen that both the present data and Castro's data are very close and are both lower than Hancock's results. It therefore appears that Hancock's argument can be extended to the case of anisotropic free-stream turbulence fields.

The Effects of Free-stream Turbulence on the Turbulence Structure of a Turbulent Boundary Layer

Huffman et al. (3) have clearly demonstrated that for nearly isotropic free-stream turbulence the turbulence properties in the boundary layer are more strongly affected by changes in the free-stream turbulence level than are any of the classical boundary layer properties. In the present experiment, the effect of anisotropic free-stream turbulence on the turbulent structure of a boundary layer is investigated. A large number of turbulence parameters within a boundary layer were measured using different kinds of hot wire probes.

Fig. 14 shows the region in the turbulence intensity-length scale plane covered by the present work. Both λ_x and λ_y for the anisotropic case are slightly larger compared to the isotropic case at the same turbulence level and the order of magnitude of λ_x and λ_y are on the same order of the boundary layer thickness.

The distribution of turbulence within the boundary layer for various levels of free-stream turbulence are shown in Fig. 15. Fig. 16 shows the turbulent kinetic energy ($2k/U_\tau^2$) distribution within the boundary layer. Note that the free-stream velocity, U_m , does not change with changes in turbulence level. It is seen from the figures that the turbulence level and turbulent kinetic energy

in the outer layer are sensitive to the free-stream turbulence, whereas the turbulence level and turbulent kinetic energy near the wall do not change appreciably with change in the free-stream turbulence. Fig. 17 shows the Reynolds stress distribution with different free-stream turbulence levels within boundary layers. Huffman indicated that the Reynolds stress and turbulent kinetic energy are largely unaffected by the free-stream turbulence level for $y/\delta \leq 0.4$; the present results agree with these findings. Consequently, it can be concluded that the inner layer shear stress producing mechanism is universal and is largely unaffected by external conditions of either isotropic or anisotropic turbulence fields.

Fig. 18 and 19 plot the distribution of three rms components of the velocity fluctuation $\sqrt{u'^2}/U_m$, $\sqrt{v'^2}/U_m$, $\sqrt{w'^2}/U_m$ within the boundary layer. The comparison of these components with different free-stream turbulence levels for near-isotropic and highly anisotropic turbulence are shown in Fig. 18a and 18b respectively. It shows that all the components of velocity fluctuations with high free-stream turbulence levels are higher than for the case of low turbulence levels in the outer part of the boundary layer. Fig. 19 shows a comparison between the highly anisotropic and near-isotropic case at the same free-stream turbulence level. It is seen that for $y/\delta > 0.4$, the $\sqrt{u'^2}/U_m$ component for anisotropic turbulence is lowest and the other components ($\sqrt{v'^2}/U_m$ and $\sqrt{w'^2}/U_m$) are higher compared to the near-isotropic case. Therefore the eddy axis generated by rod sets and the contraction of the channel make a contribution to isotropy.

CONCLUSIONS

The effect of anisotropic free-stream turbulence level on the classic boundary layer properties: i.e., δ , δ^*/δ , H , $\Delta H/H_0$, c_f , $\Delta c_f/c_{f0}$, can be summarized as follows:

1. The present results of the effect of anisotropic free-stream turbulence level on the classic boundary layer properties are similar to those of other recent works for isotropic turbulence, i.e., (a) boundary layer thickness and skin friction increase with increasing turbulence level; (b) the mean velocity nondimensionalized with U_τ remains largely unchanged in inner region of the boundary layer; however, there is a marked reduction in the wake component as the free-stream turbulence level increase; and (c) the shape factor H decreases with increased turbulence level due to the reduced wake-component.
2. The present experimental results confirms both the results of recent published papers by Hancock (5) and Castro (7), i.e., the effect of free-stream turbulence decreases with increasing free-stream length scale, and momentum thickness Reynolds number has a significant effect when the $Re_\theta < 2000$.

The effects of free-stream turbulence on the structure of a turbulent boundary layer reveal a different influence for near-isotropic and highly anisotropic free-stream turbulence fields.

1. The turbulence level and Reynolds stress distributions within the boundary layer are sensitive to free-stream turbulence in the outer part of the boundary layer, and are largely unaffected in the inner layer.
2. The velocity fluctuation components in the outer part of the boundary layer for anisotropic free-stream turbulence have quite different rms values compared to the near-isotropic case. The longitudinal fluctuation component, generally, is lower for highly anisotropic free-stream turbulence compared to the isotropic turbulence case, while the lateral and normal fluctuation components are much higher compared to the near-isotropic case. Thus, the advection of the free-stream turbulent energy has directivity in the outer part of boundary layer.

ACKNOWLEDGEMENT

The authors gratefully acknowledge the support of this investigation by NASA-ARC through Grant NSG-2391.

BIBLIOGRAPHY

1. Parikh, P. G., Reynolds, W. C. and Jayaraman, R., "Behavior of an Unsteady Turbulent Boundary Layer." AIAA Journal, Vol. 20, No. 6, June 1982, pp. 764-775.
2. Kline, S. J., Lisin, A. V. and Waitman, B. A., "Preliminary Experimental Investigation of Effects of Free-Stream Turbulence on Turbulent Boundary Layer Growth." NASA TN D-368, 1960.
3. Huffman, G. D., Zimmerman, D. R. and Bennett, W. A., "The Effect of Free-Stream Turbulence Level on Turbulent Boundary Layer Behavior." AGARD, No. 164 on Boundary Layer Effects in Turbomachines, edited by J. Surugus, April, 1972.
4. Meier, H. U. and Kreplin, H. P., "Influence of Free-Stream Turbulence on Boundary Layer Development." AIAA Journal, Vol. 18, 1981, p. 11.
5. Hancock, P. E. and Bradshaw, P., "The Effect of Free-Stream Turbulence on Turbulent Boundary Layers." ASME Journal of Fluids Engineering, Vol. 105, September 1983, p. 284.
6. Raghunathan, S. and McAdam, R. J. W., "Free-Stream Turbulence Effects on Attached Subsonic Turbulent Boundary Layer." AIAA Journal, Vol. 21, No. 4, 1983.
7. Castro, I. P., "Effects of Free-Stream Turbulence on Low Reynolds Number Boundary Layers." ASME Journal of Fluids Engineering, Vol. 106, September 1984.
8. Sullerey, R. K. and Sayeed Khan, M. A., "Free-Stream Turbulence Effects on Compressor Cascade Wake." Journal of Aircraft, Vol. 20, No. 8, 1983.
9. Head, M. R. and Rechenberg, I., "The Preston Tube as a Means of Measuring Skin Friction." Journal of Fluid Mechanics, Vol. 14, 1962.
10. Green, J. E., "On the Influence of Free-Stream Turbulence on a Turbulent Boundary Layer as it Relates to Wind Tunnel Testing at Subsonic Speeds." AGARD Report 602, 1973.

TABLE 1

Geometrical Upstream Rod Sets and Grid Sets

Grid Set	B/W_1	B/M	n	S/W_1	r/W_1
1	0.034	0.108	screen	0.12	
2	0.122	0.25	3 x 11	0.12	
3	0.122	0.31	3 x 13	0.12	
4	0.176	0.36	3 x 11	0.12	
5	0.244	0.40	5 x 14	0.06	
6	0.305	0.353	4 x 10	0.12	
7	0.351	0.332	1 x 7	0.12	
Rod Set	D/W_1	D/M	n	S/W_1	r/W_1
1	0.092	0.27	32		4.62
2	1.28	0.57	7		5.51
3	3.03	0.74	5		7.32
4	3.9	0.61	5		9.76
5	5.9	0.71	4		11.2

TABLE 2

Summary of Results

Grid Set or Rod Set	$\sqrt{q^2/U_m}$ (%)	δ (m.m.)	δ^2/δ	θ/δ	H	C_f	Re_θ	U (m/s)	$\sqrt{u^2/U_H}$ (%)	$\sqrt{v^2/u}$	$\sqrt{w^2/u}$	λ_x/δ	k
None	0.48	3.00	0.1095	0.0819	1.34	0.00346	738	1.95					
Grid Set													
1	1.51	4.00	0.097	0.076	1.275	0.00373	776	1.97	1.14	1.62	1.29	0.61	0.719
2	3.16	6.50	0.0912	0.0729	1.257		920		3.42	0.957	0.807	0.49	3.13
3	4.83	5.00	0.0816	0.0655	1.242	0.00396	1063	2.03	4.40	1.28	0.986	0.60	5.27
4	5.50	5.50	0.0714	0.0584	1.223	0.0040	1017	2.04	5.20	1.13	1.12	0.60	9.98
5	6.30	5.80	0.055	0.0461	1.194	0.00406	900	2.06	4.80	1.49	1.35	0.635	12.20
6	7.50	7.50	0.0506	0.0431	1.172	0.0042	977	2.10	6.30	1.29	1.26	0.75	17.61
7	8.10	8.50	0.0537	0.0449	1.197		875		8.25	0.96	1.00	0.93	20.70
Rod Set													
1	2.02	3.60	0.0903	0.0700	1.29	0.00373	757	1.97	0.98	2.62	2.21	0.80	1.28
2	2.92	4.80	0.0757	0.0606	1.248	0.00378	838	1.99	1.29	3.08	2.92	0.875	3.31
3	3.82	5.60	0.0676	0.0547	1.236	0.00385	854	2.01	2.07	2.53	1.67	0.850	4.51
4	4.98	6.50	0.0577	0.0475	1.213	0.00393	870	2.03	2.31	3.03	2.00	0.805	7.767
5	7.10	8.00	0.0523	0.0439	1.19	0.00414	1055	2.08	3.19	3.09	2.26	0.854	16.61

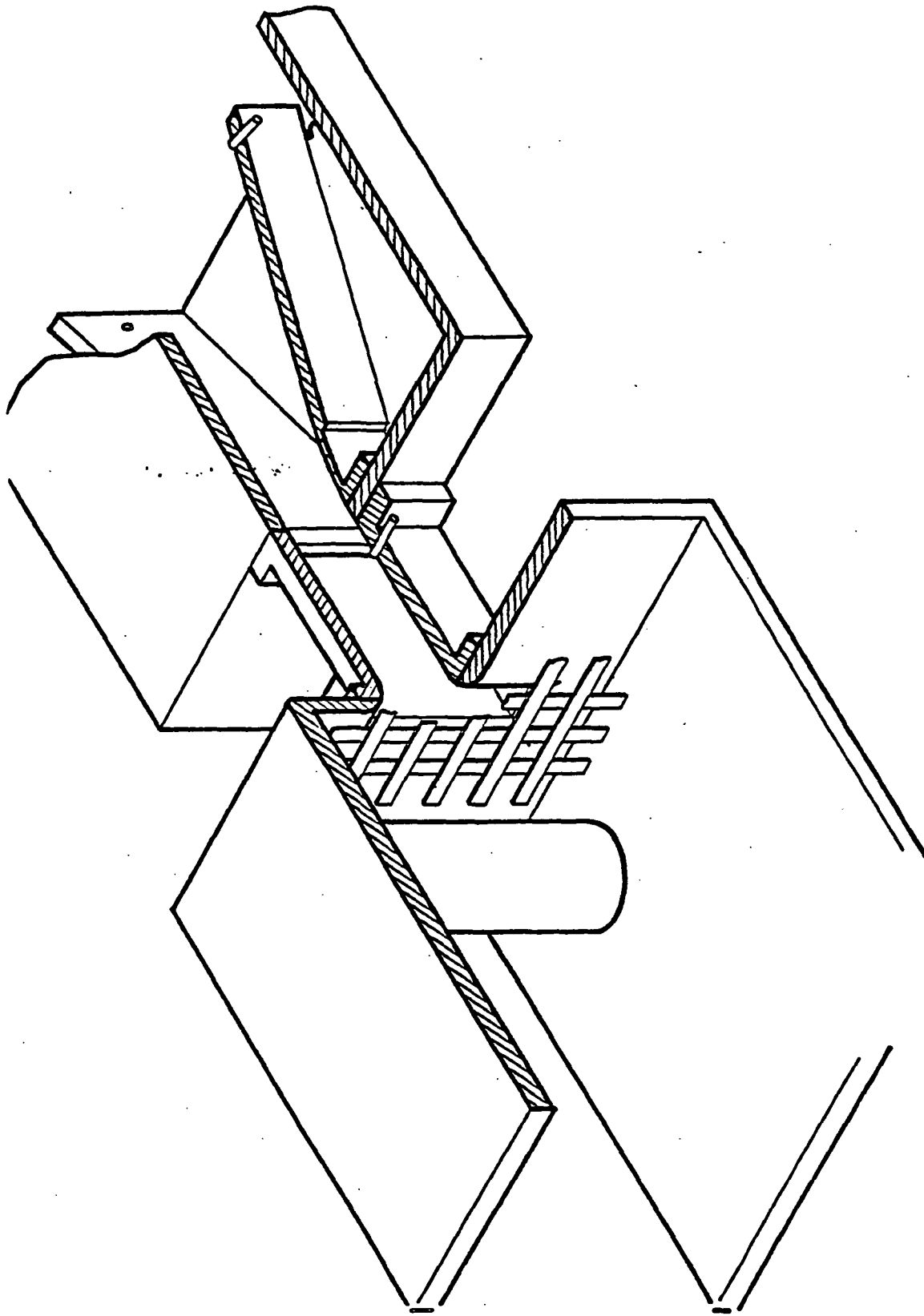


Fig. 1a
Experiential System Schematic

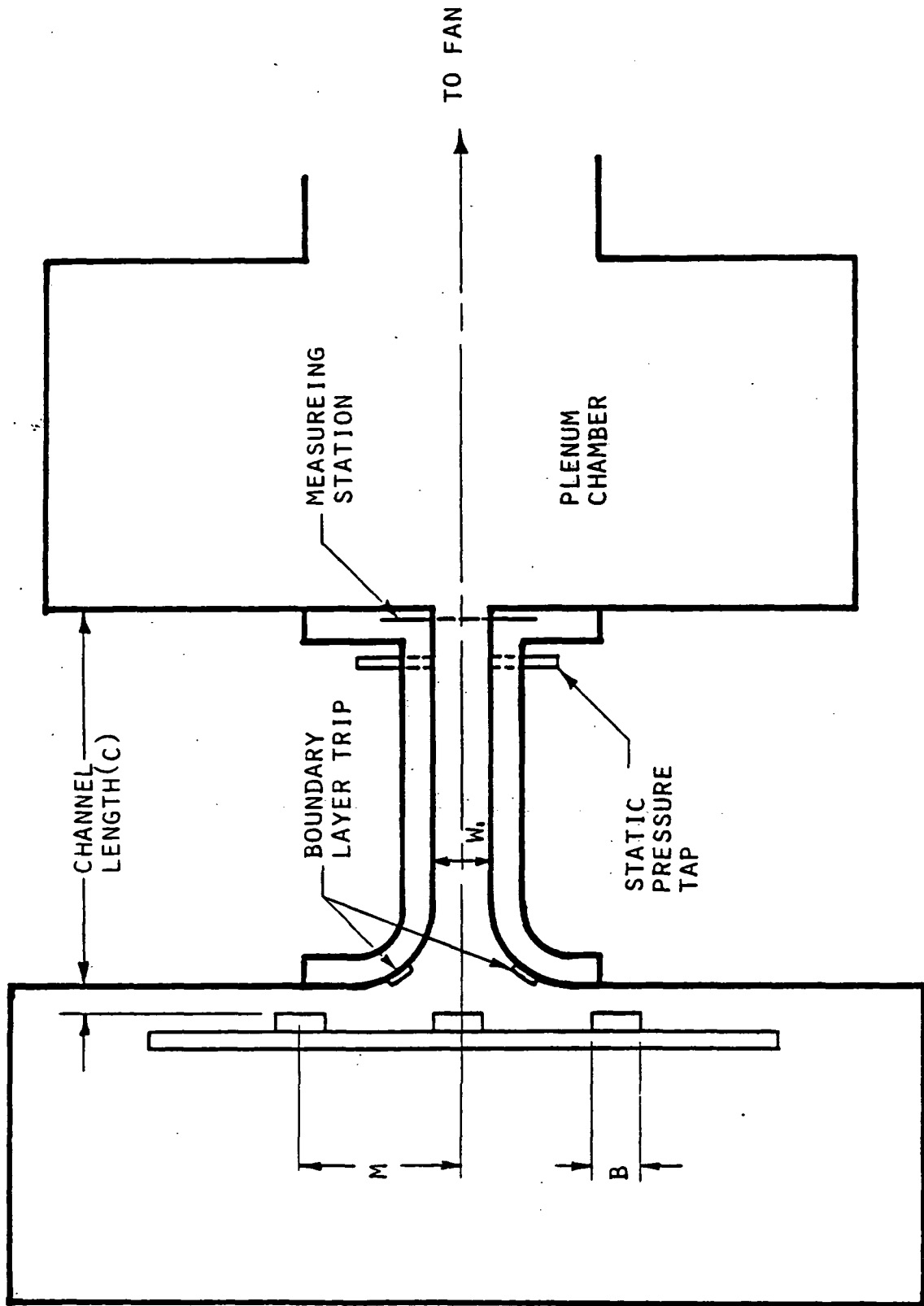


FIG. 1b. EXPERIMENTAL SYSTEM SECTION

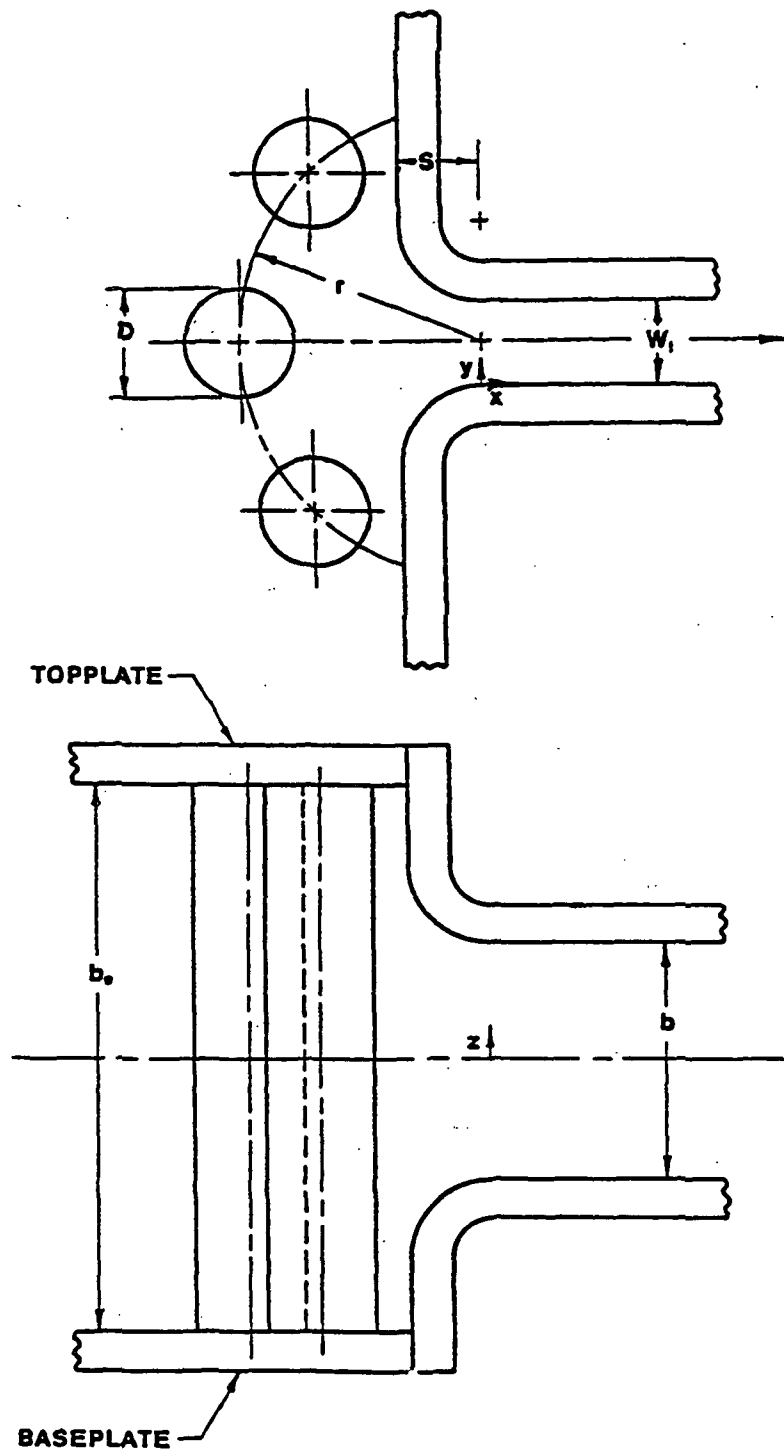


Fig. 2

Rod Set Geometry Nomenclature

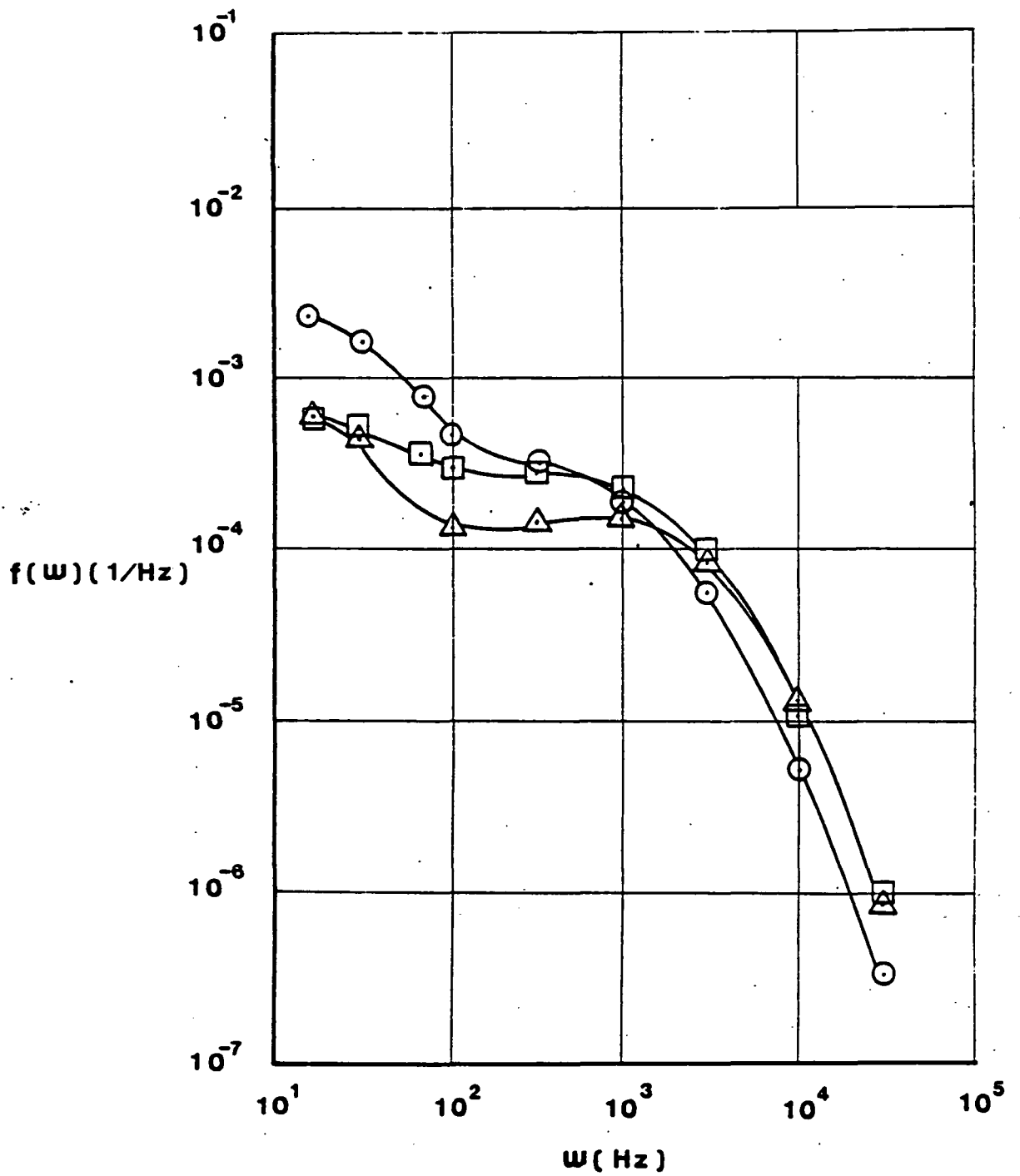


Fig. 3

Spectral Density Curves of Inlet Free-Stream Turbulence
with Three Different Rod Sets

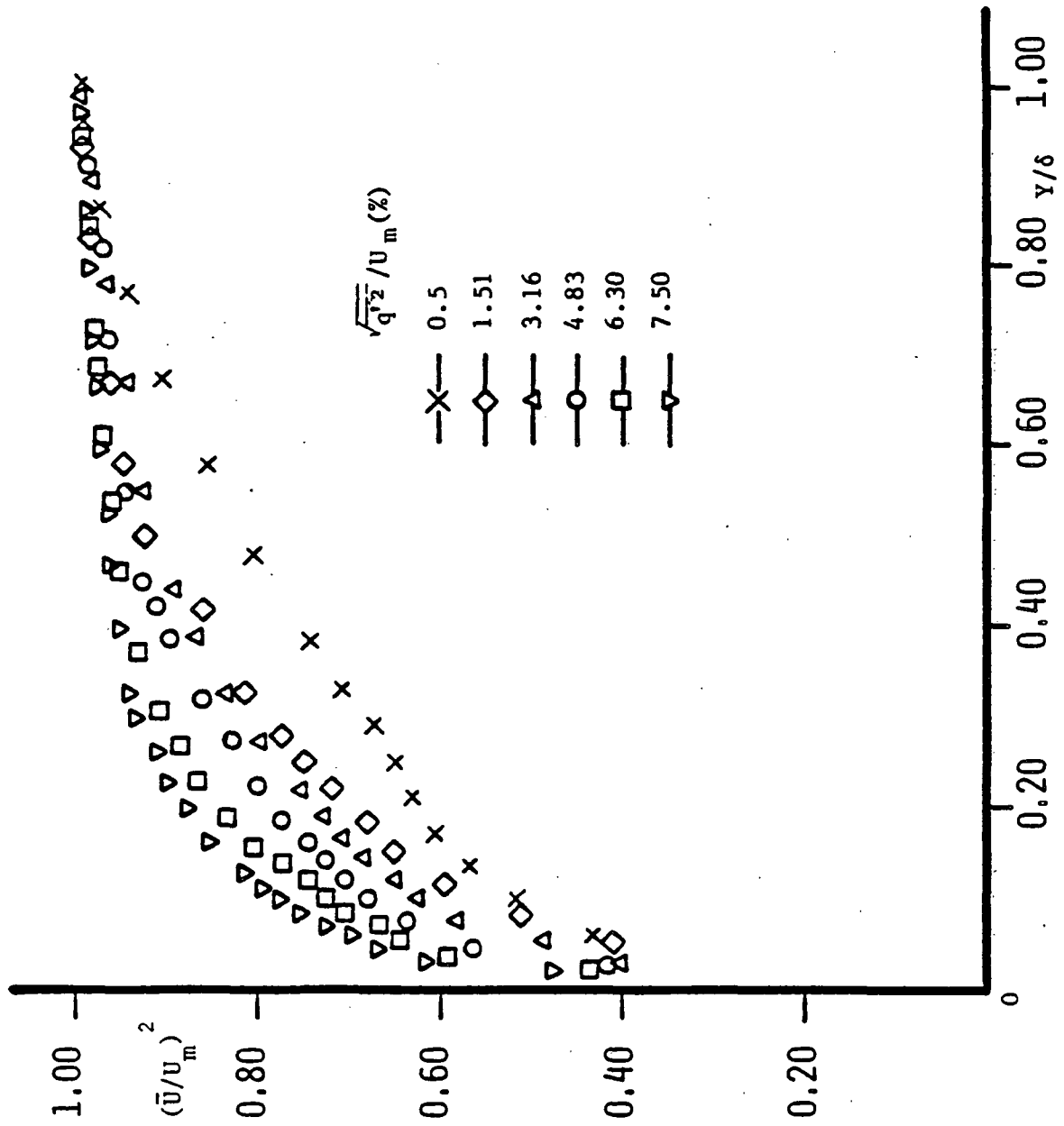


FIG. 4 NONDIMENSIONAL VELOCITY RATIO PARAMETER FOR VARIOUS FREE-STREAM TURBULENCE LEVELS

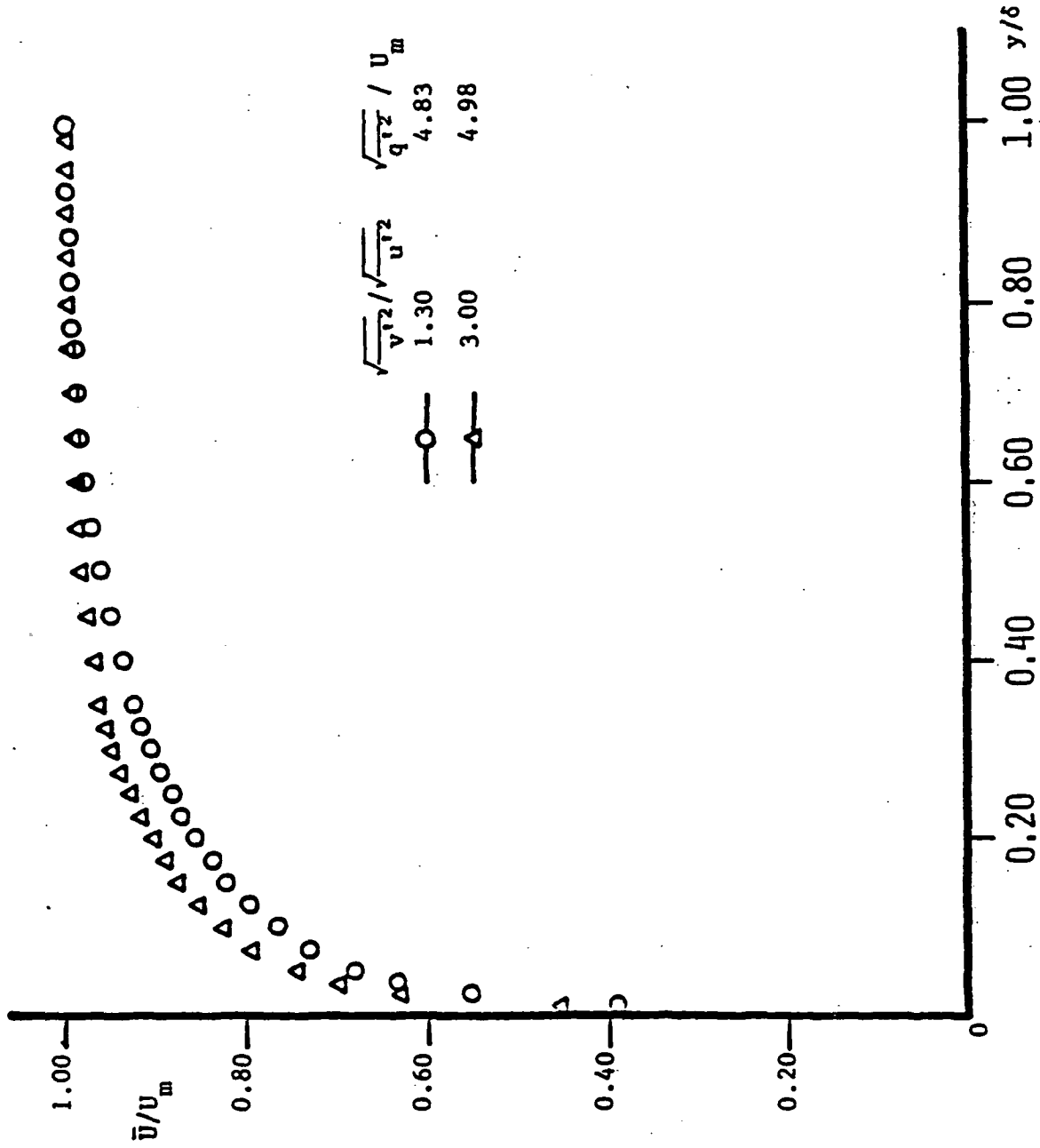


FIG. 5 NONDIMENSIONAL VELOCITY PROFILES FOR NEARLY ISOTROPIC AND
 HIGHLY ANISOTROPIC FREE-STREAM TURBULENCE WITH NEAR EQUAL
 TOTAL TURBULENCE LEVEL

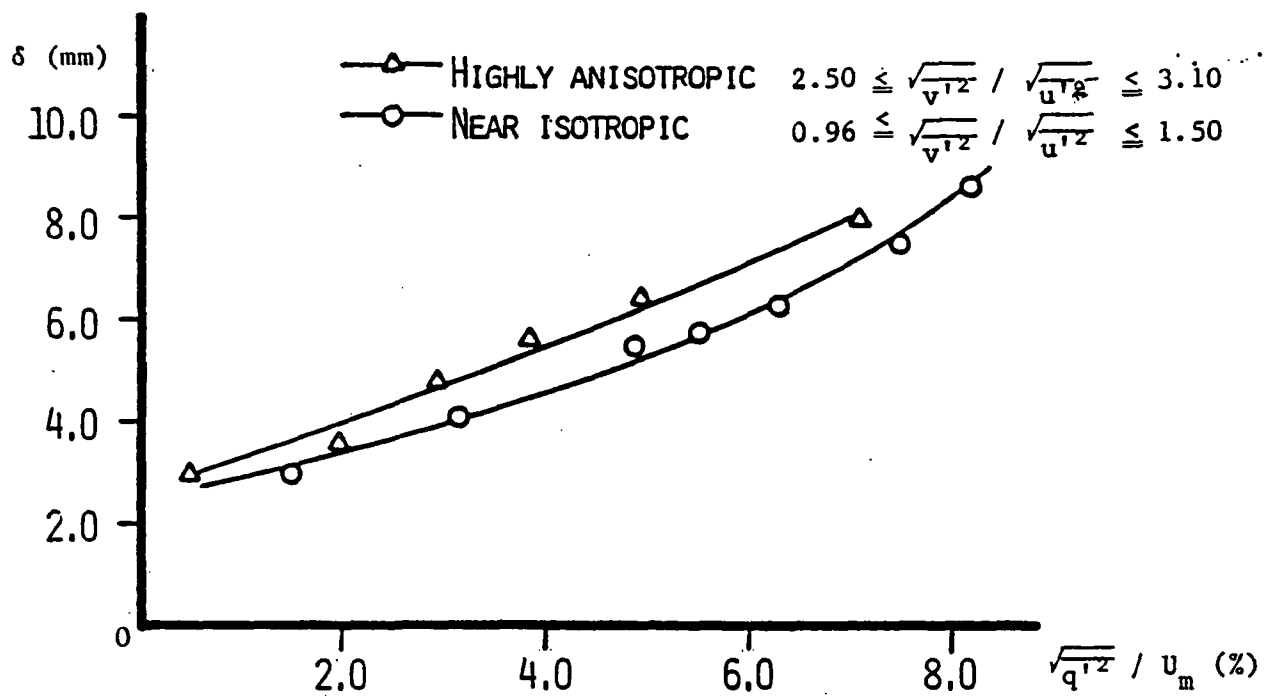


FIG.6 VARIATION OF BOUNDARY LAYER THICKNESS WITH FREESTREAM TURBULENCE

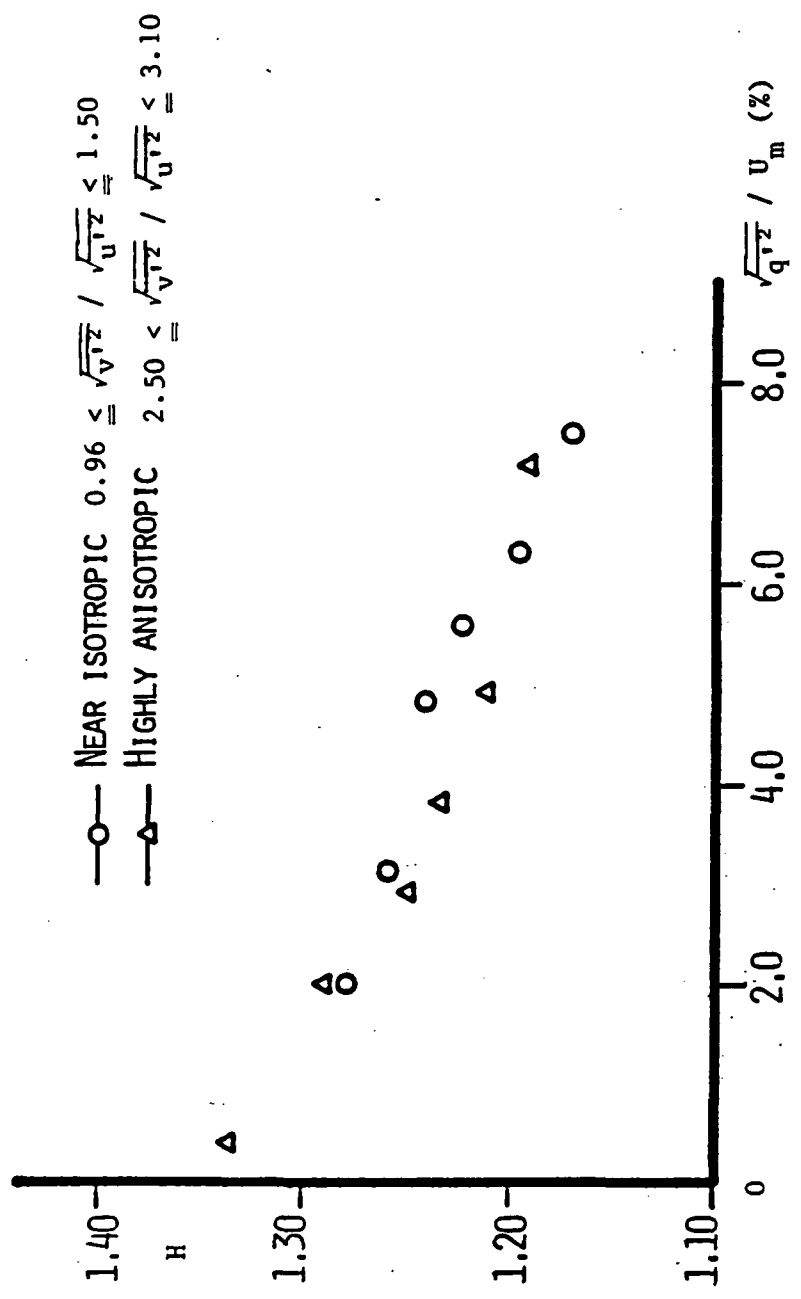


FIG. 7 VARIATION IN BOUNDARY LAYER SHAPE FACTOR VERSUS $\frac{\sqrt{q}}{\sqrt{u}} / \frac{\sqrt{q}}{\sqrt{u}}$

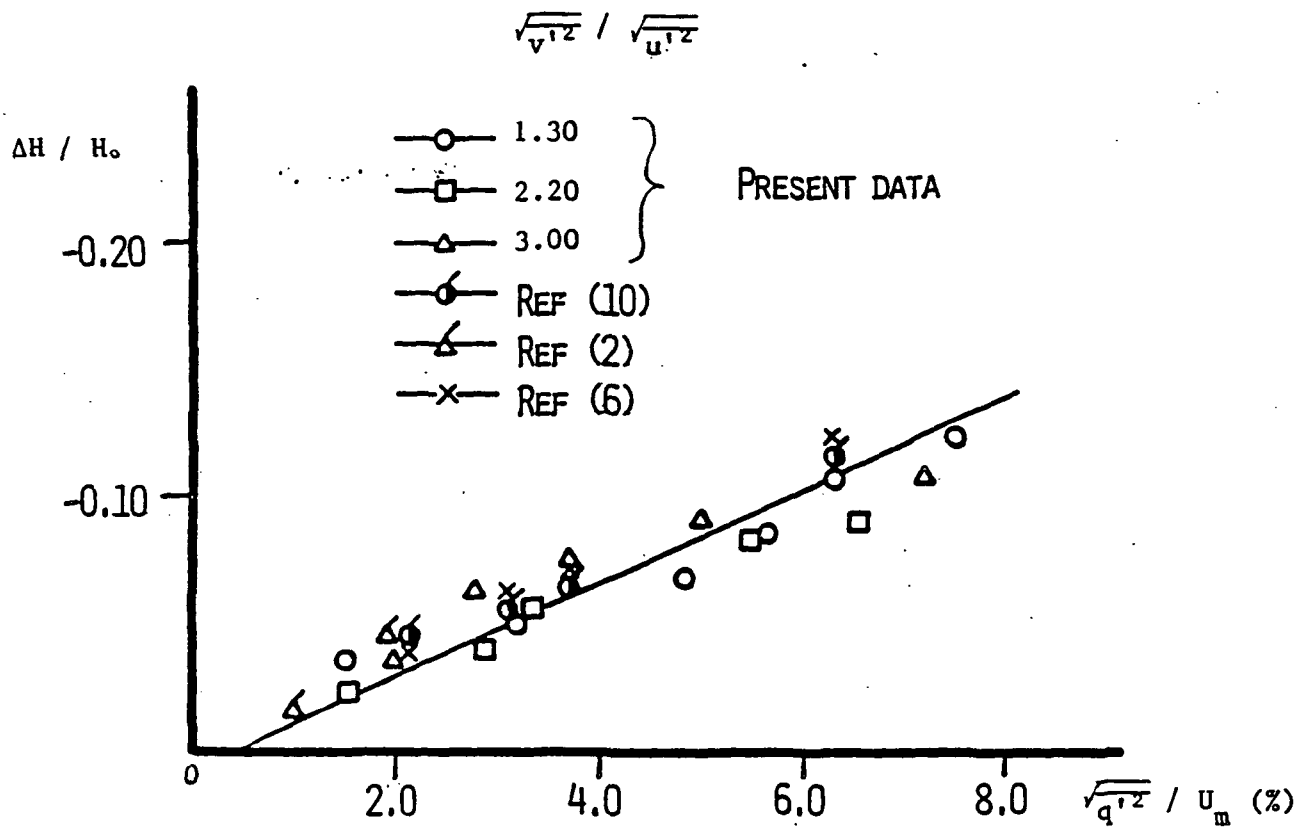


FIG. 8 INFLUENCE OF $\frac{\sqrt{q'^2}}{U_m}$ ON $\Delta H / H_0$.

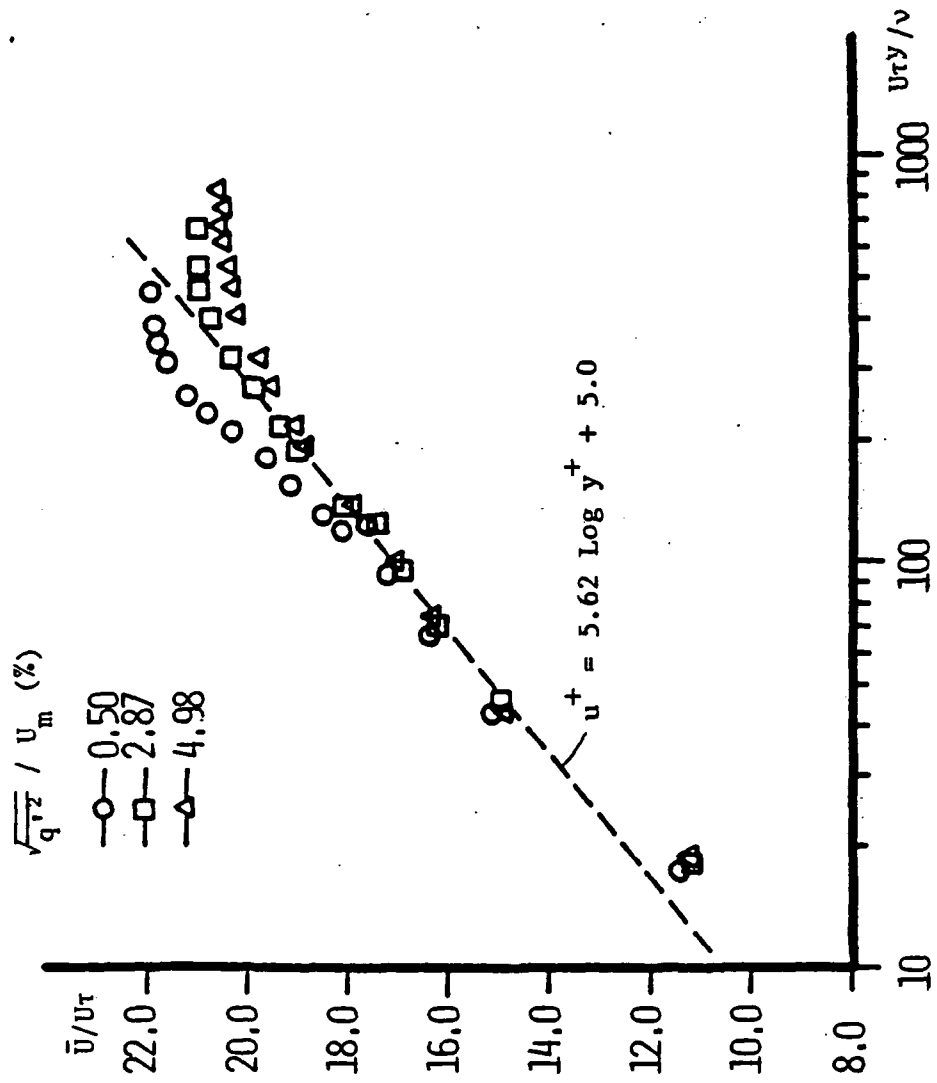


FIG. 9 VARIATION IN LAW OF THE WALL PLOTS

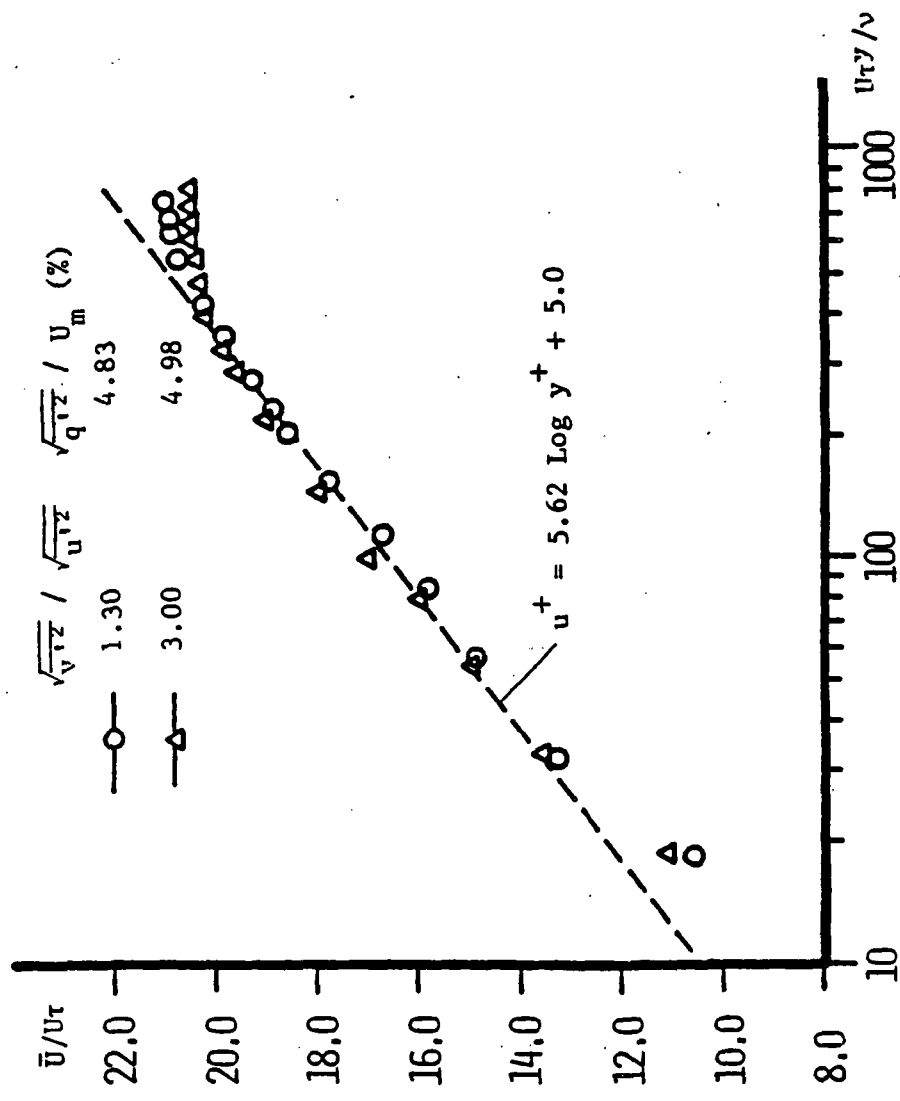


FIG. 10 VARIATION IN LAW OF WALL PLOTS

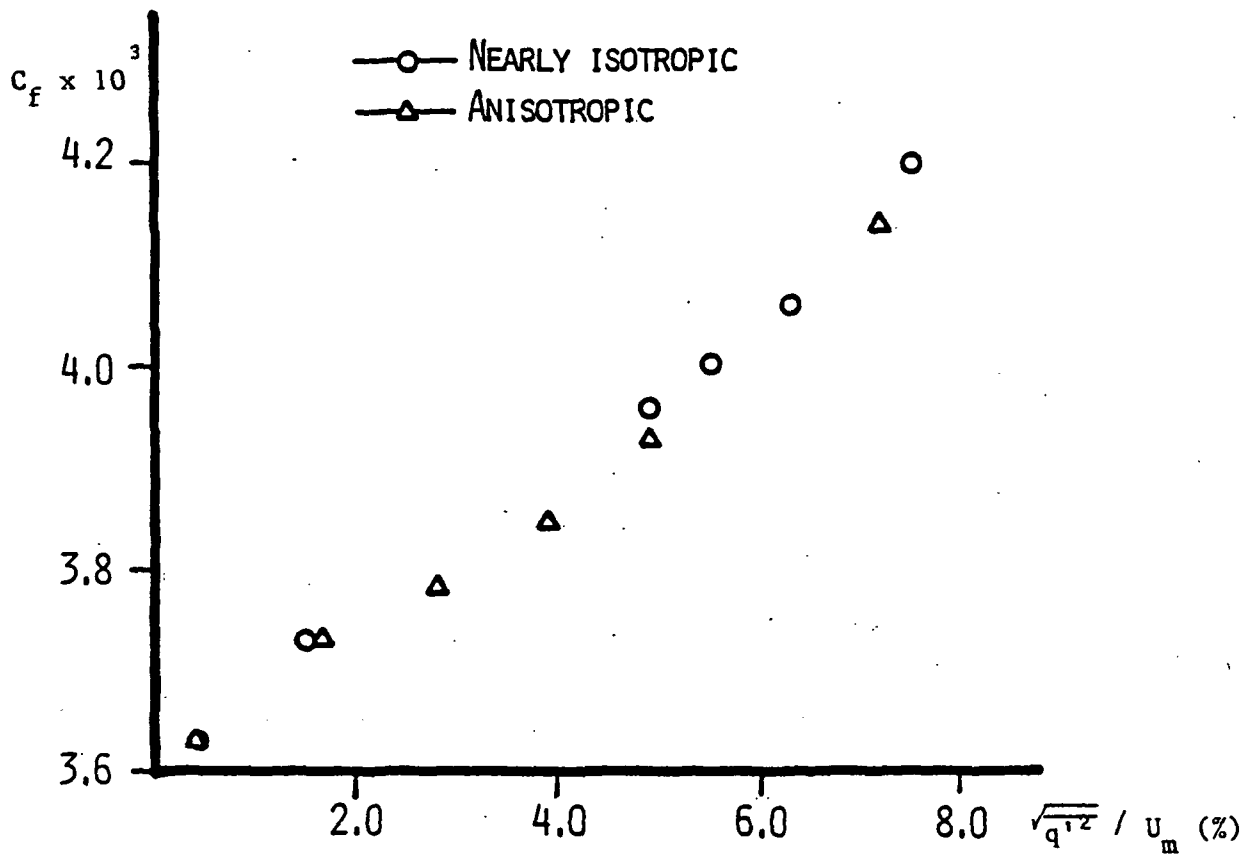


FIG. 11 VARIATION OF SKIN FRICTION WITH $\sqrt{q'^2} / U_m$

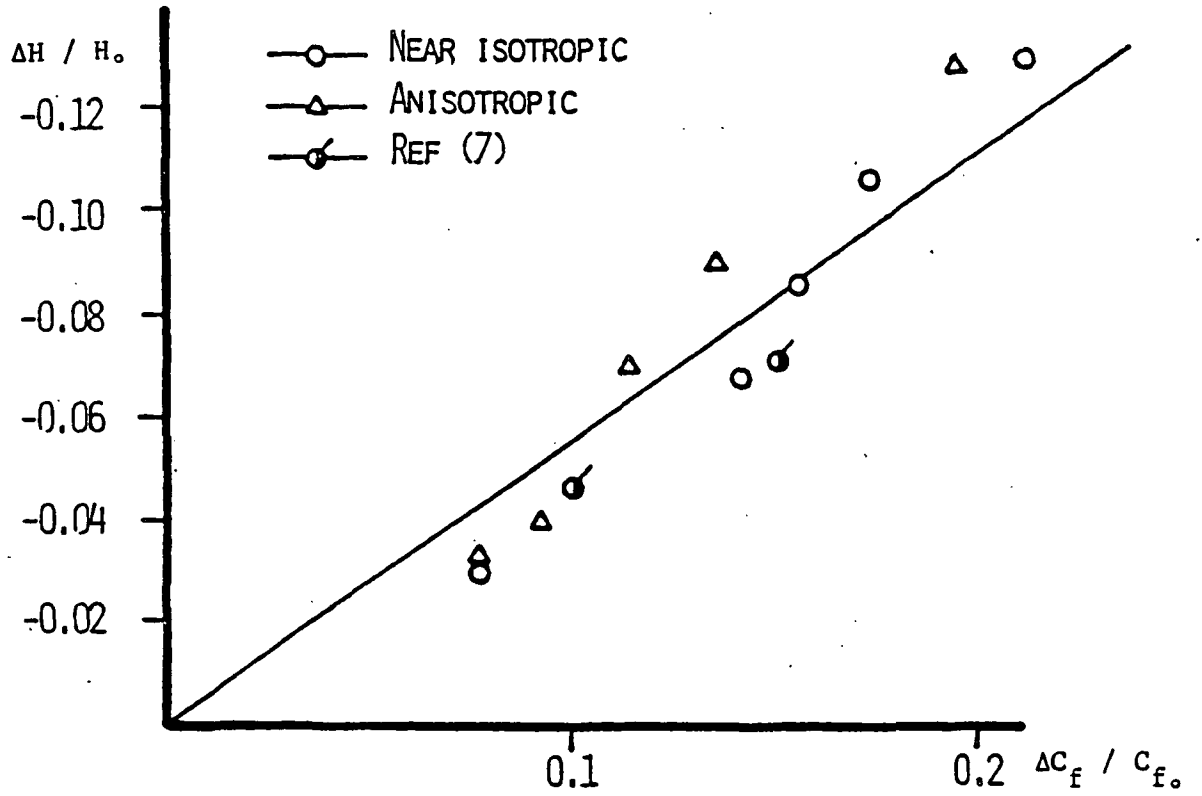


FIG. 12 CORRELATION BETWEEN FRACTIONAL INCREASE IN SHAPE FACTOR H WITH $\Delta C_f / C_{f_0}$.

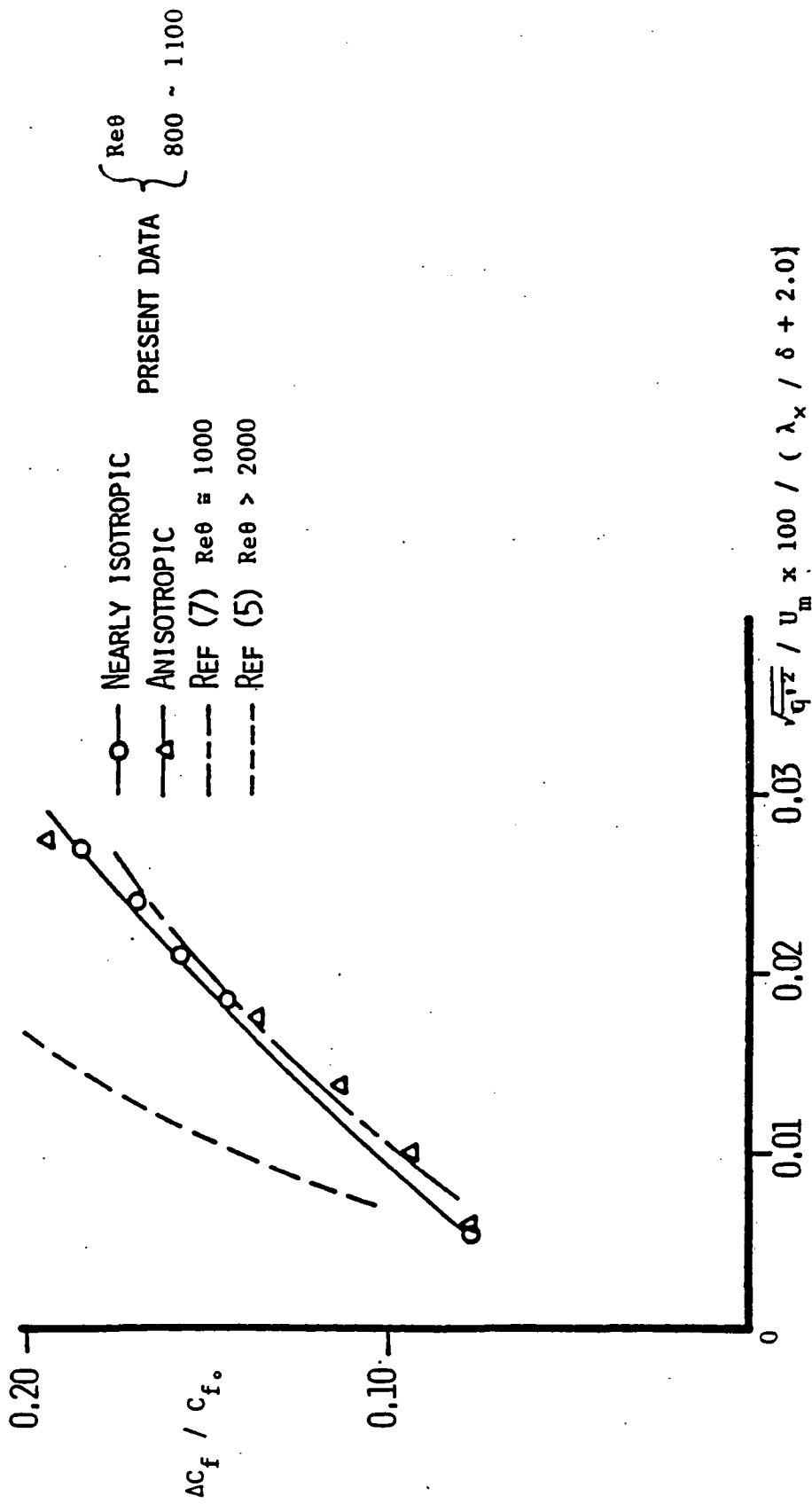


Fig. 13 CORRELATION OF FRACTIONAL CHANGE IN SKIN FRICTION COEFFICIENT AS A FUNCTION OF FREE-STREAM TURBULENCE LEVEL AND LENGTH SCALE

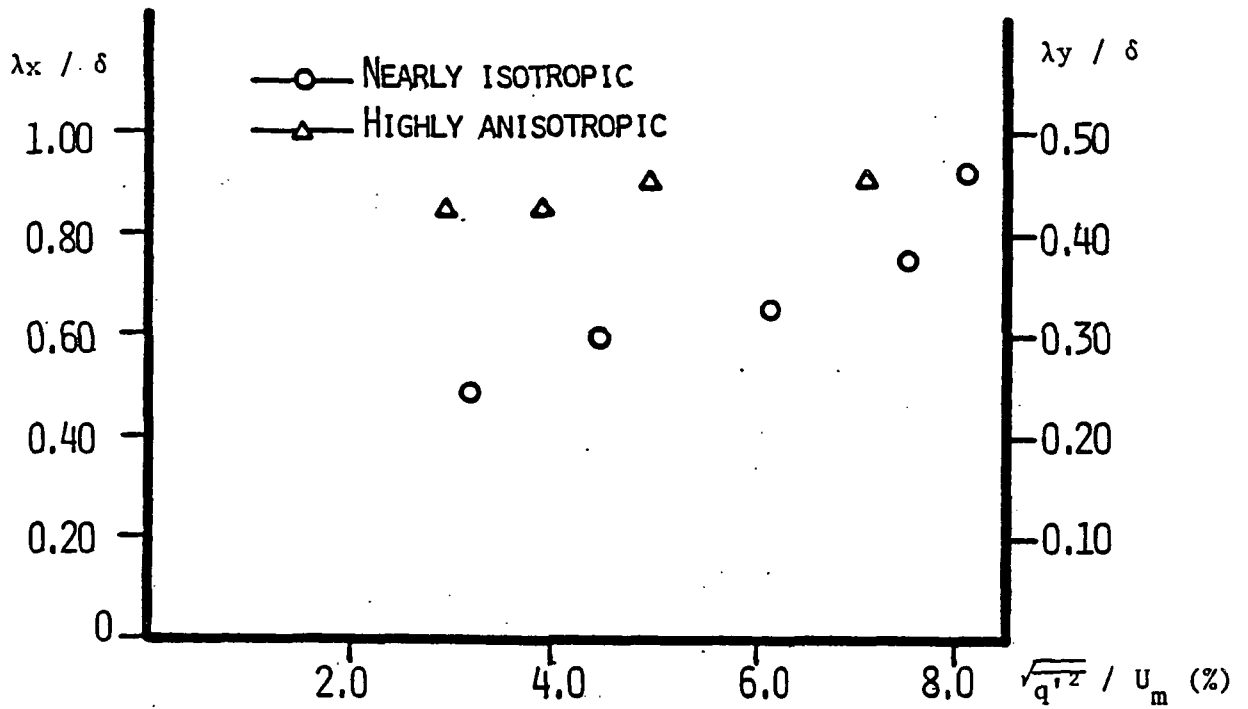


FIG. 14 FREE-STREAM TURBULENCE LEVEL AND LENGTH SCALE RATIO RANGE COVERED BY PRESENT WORK

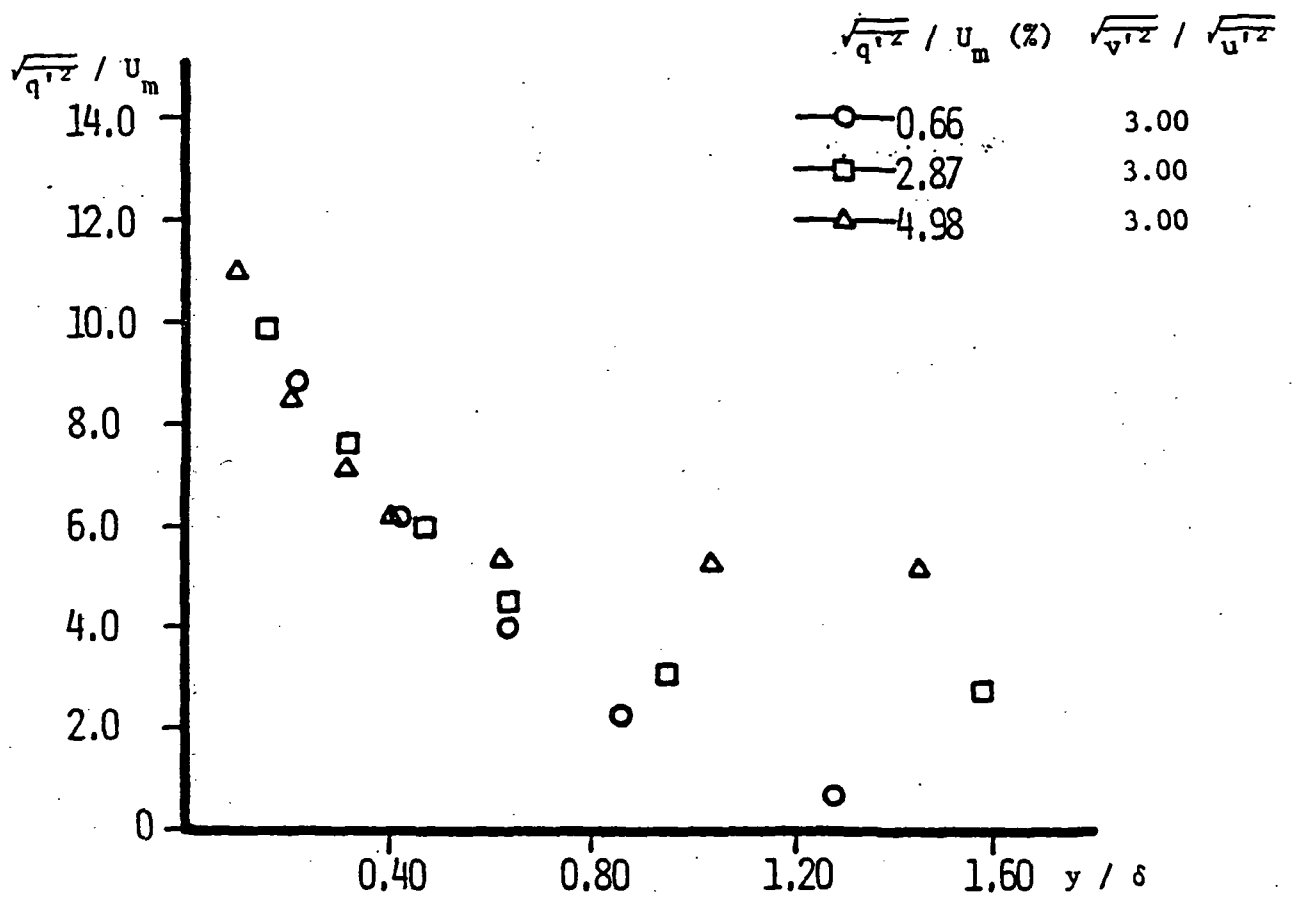


FIG. 15A DISTRIBUTION OF TUBULENCE WITHIN THE BOUNDARY LAYER FOR DIFFERENT FREE-STREAM LEVELS OF ANISOTROPIC TURBULENCE

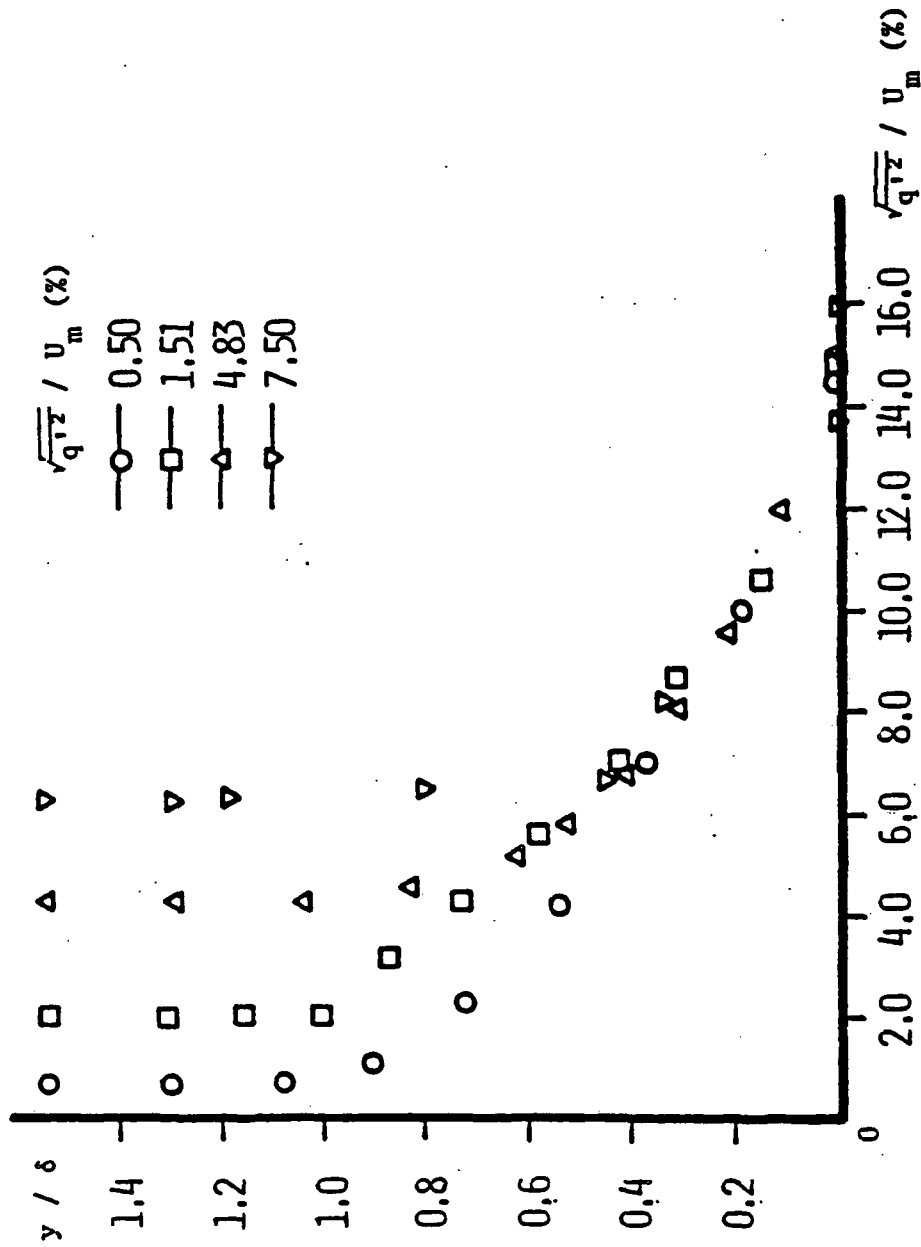


FIG. 15B DISTRIBUTION OF TURBULENCE WITH THE BOUNDARY LAYER FOR
 DIFFERENT FREE-STREAM LEVELS WITH $\sqrt{v^{12}} / \sqrt{u^{12}} = 1.30$

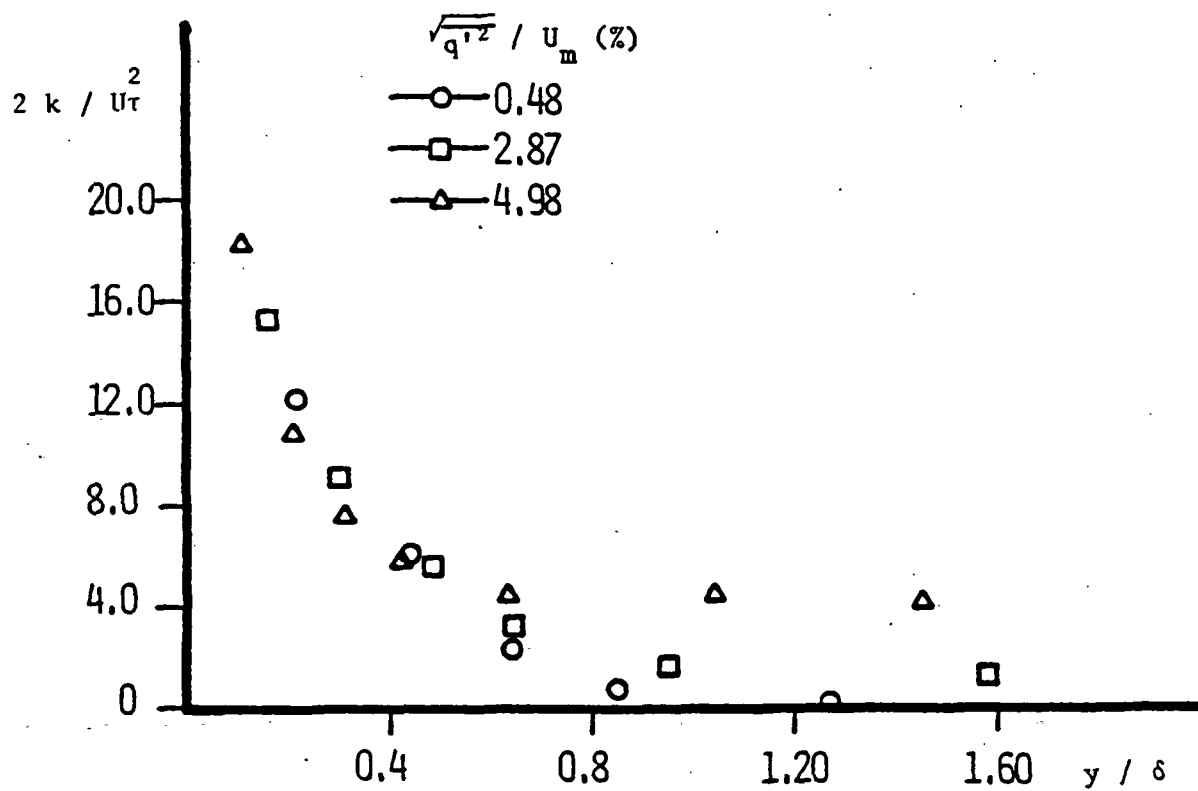


FIG. 16 TURBULENT KINETIC ENERGY DISTRIBUTION WITHIN
 BOUNDARY LAYERS

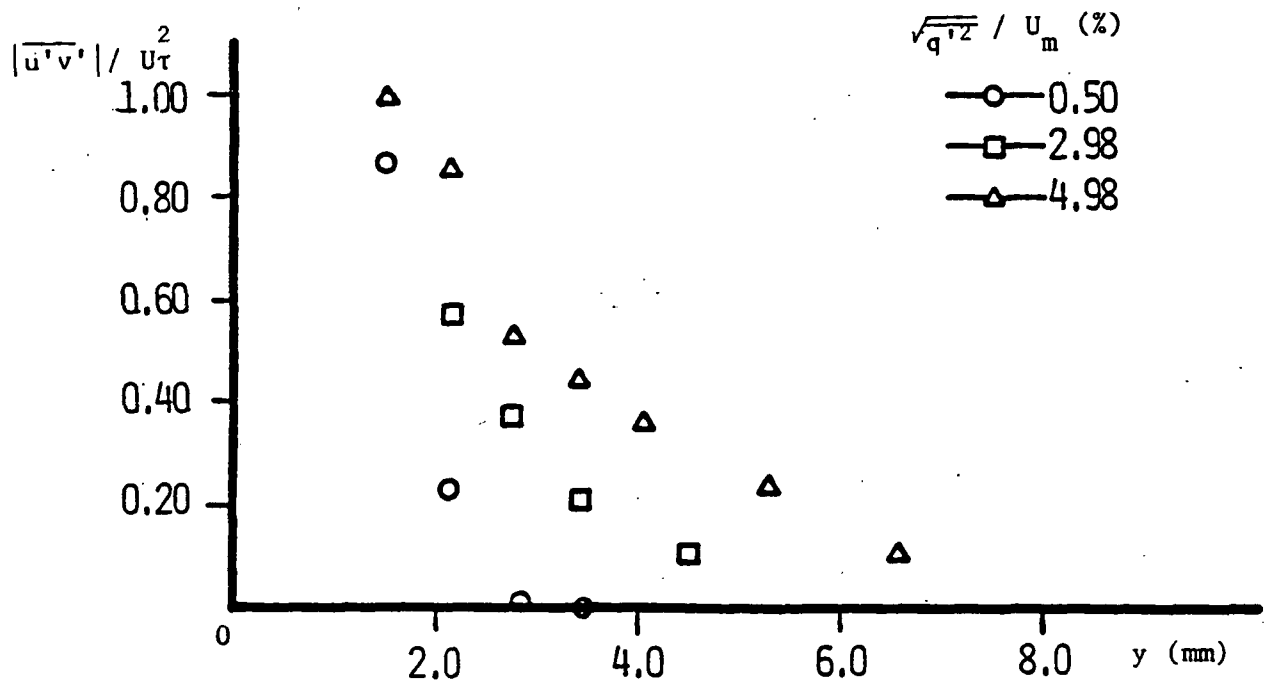


FIG. 17 REYNOLDS STRESS AS A FUNCTION OF POSITION

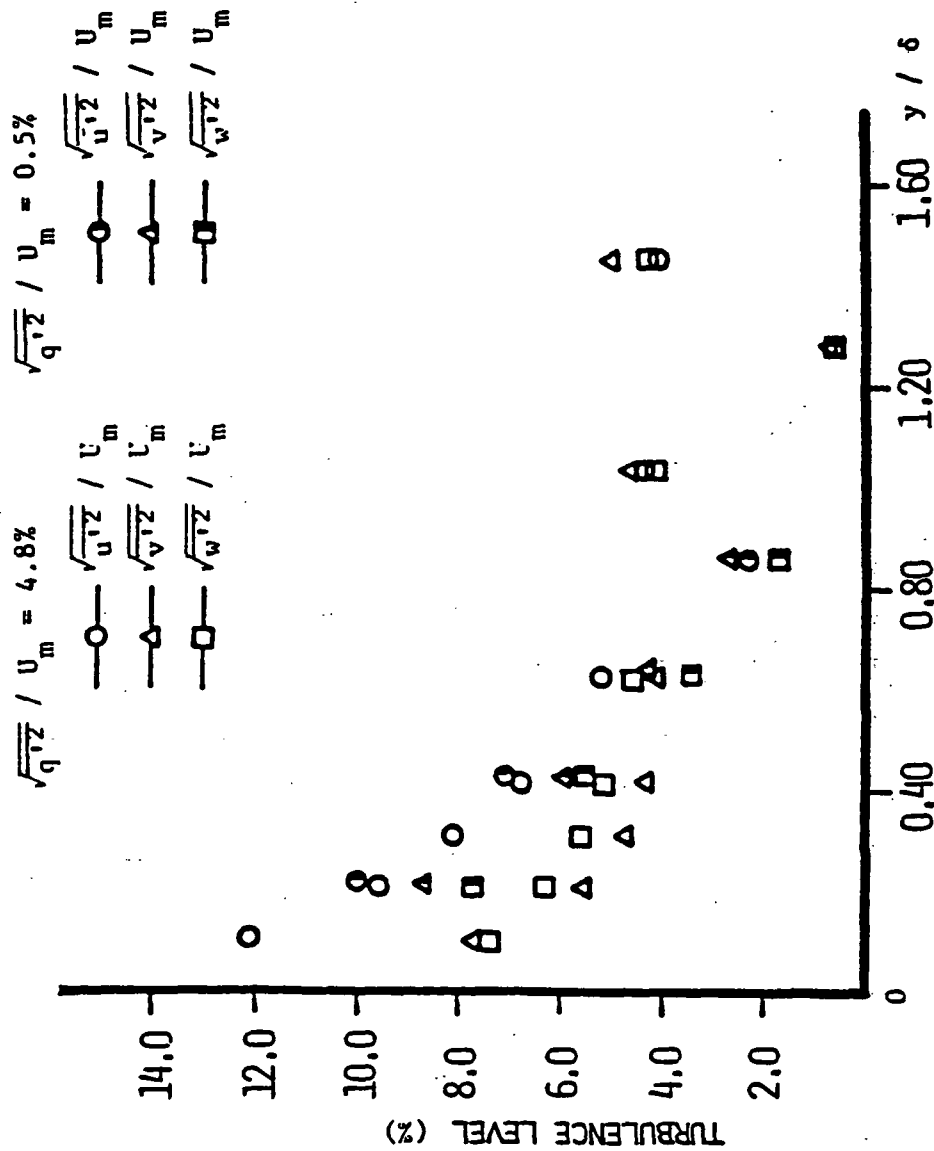


FIG. 18A TURBULENCE LEVEL DISTRIBUTION OF THREE VELOCITY COMPONENTS WITHIN BOUNDARY LAYER FOR NEAR ISOTROPIC FREE-STREAM TURBULENCE

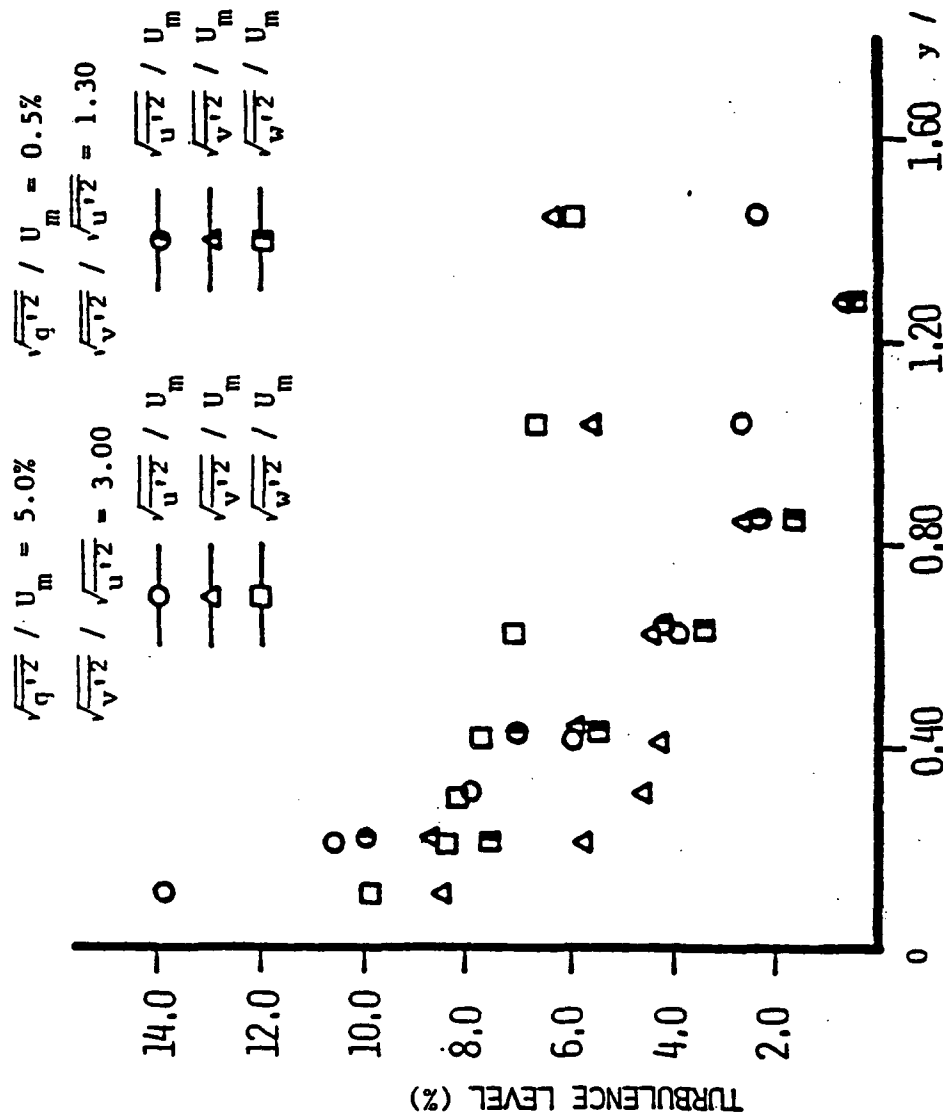


Fig. 18B TURBULENCE LEVEL DISTRIBUTION OF THREE VELOCITY COMPONENTS WITHIN BOUNDARY LAYER FOR ANISOTROPIC FREE-STREAM TURBULENCE

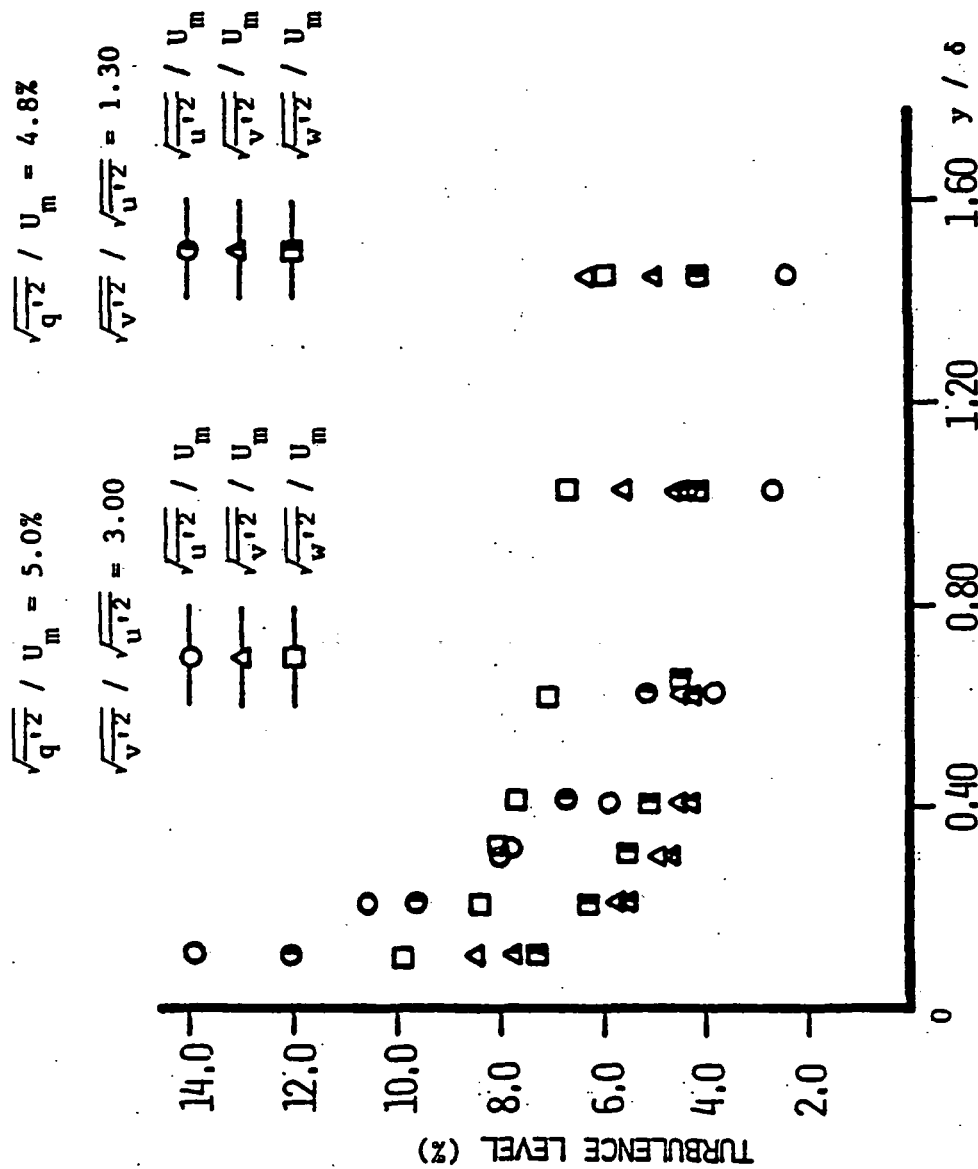


FIG. 19 TURBULENCE LEVEL DISTRIBUTION OF THREE VELOCITY COMPONENTS
 WITHIN BOUNDARY LAYER FOR NEAR ISOTROPIC AND HIGHLY ANISOTROPIC
 FREE-STREAM TURBULENCE AT NEAR EQUAL FREE-STREAM TURBULENCE LEVELS

1. Report No. CR - 177379	2. Government Accession No.	3. Recipient's Catalog No.	
4. Title and Subtitle "The Effects of Anisotropic Free-Stream Turbulence on Turbulent Boundary Layer Behavior		5. Report Date November 1985	6. Performing Organization Code
		8. Performing Organization Report No.	
7. Author(s) Fang Liang-Wei and Jon A. Hoffman		10. Work Unit No. T-7526	
9. Performing Organization Name and Address California Polytechnic State University San Luis Obispo, CA 93407		11. Contract or Grant No. NSG-2391	
		13. Type of Report and Period Covered Contractor Report 7-1-84 to 7-1-85	
12. Sponsoring Agency Name and Address National Aeronautics and Space Administration Washington, D.C. 20546		14. Sponsoring Agency Code 505-61-71	
		15. Supplementary Notes Technical Monitor: David G. Koenig & Michael Dudley, Mail Stop 247-1 NASA Ames Research Center, Moffett Field, CA 94035, Phone: 415) 694-5046	
16. Abstract <p>The effects of near-isotropic and highly anisotropic free-stream turbulence on mean flow properties and properties of the turbulent structure of turbulent boundary layers in a near zero pressure gradient flow has been experimentally evaluated. Turbulence levels varied from 0.5% to 8.0% and the momentum thickness Reynolds number varied from 800 to 1100.</p> <p>The results indicate that the effects of free-stream turbulence on the classical boundary layer properties for near -isotropic turbulence which have been published by other investigators are similar to the case of highly anisotropic turbulence fields, while the effects of free-stream turbulence on the properties of the turbulent structure within the boundary layer for the case of near-isotropic turbulence are quite different compared to the highly anisotropic case.</p>			
17. Key Words (Suggested by Author(s)) boundary layer, turbulence, performance		18. Distribution Statement Subject category - 02 Unclassified - Unlimited	
19. Security Classif. (of this report) Unclassified	20. Security Classif. (of this page) 0	21. No. of Pages 38	22. Price*